INL/EXT-10-20619

Modeling a Printed Circuit Heat Exchanger with RELAP5-3D for the Next Generation Nuclear Plant

Prashaanth Ravindran
Piyush Sabharwall
Nolan A. Anderson

December 2010

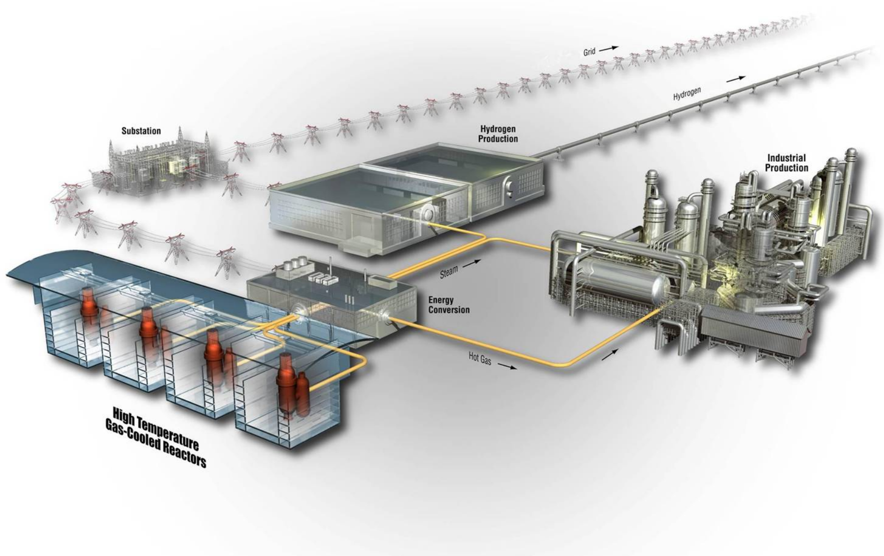

The INL is a
U.S. Department of Energy
National Laboratory
operated by
Battelle Energy Alliance

Idaho National Laboratory

INL/EXT-10-20619

Modeling a Printed Circuit Heat Exchanger with RELAP5-3D for the Next Generation Nuclear Plant

Prashaanth Ravindran
Piyush Sabharwall
Nolan A. Anderson

December 2010

Idaho National Laboratory
Next Generation Nuclear Plant Project
Idaho Falls, Idaho 83415

Prepared for the
U.S. Department of Energy
Office of Nuclear Energy
Under DOE Idaho Operations Office
Contract DE-AC07-05ID14517

Next Generation Nuclear Plant Project

Modeling a Printed Circuit Heat Exchanger with RELAP5-3D for the Next Generation Nuclear Plant

INL/EXT-10-20619

December 2010

Approved by:

Piyush Sabharwall NGNP Advance Heat Transport Lead	12-9-10 Date
Nolan A. Anderson Thermal Fluids and Safety Analysis Engineer	12-9-10 Date
Michael W. Patterson Hydrogen Process & Heat Transport Systems Program Manager	12/9/2010 Date

ABSTRACT

The main purpose of this report is to design a printed circuit heat exchanger (PCHE) for the Next Generation Nuclear Plant and carry out Loss of Coolant Accident (LOCA) simulation using RELAP5-3D. Helium was chosen as the coolant in the primary and secondary sides of the heat exchanger. The design of PCHE is critical for the LOCA simulations. For purposes of simplicity, a straight channel configuration was assumed. A parallel intermediate heat exchanger configuration was assumed for the RELAP5 model design. The RELAP5 modeling also required the semicircular channels in the heat exchanger to be mapped to rectangular channels. The initial RELAP5 run outputs steady state conditions which were then compared to the heat exchanger performance theory to ensure accurate design is being simulated.

An exponential loss of pressure transient was simulated. This LOCA describes a loss of coolant pressure in the primary side over a 20 second time period. The results for the simulation indicate that heat is initially transferred from the primary loop to the secondary loop, but after the loss of pressure occurs, heat transfers from the secondary loop to the primary loop.

ACKNOWLEDGEMENTS

The authors are thankful to Mr. Cliff B. Davis and Mr. Paul D. Bayless for their invaluable assistance and time towards this project. The authors extend their gratitude to Mike Patterson for his advice and assistance.

CONTENTS

FIGURES

TABLES

ACRONYMS

ASME	American Society of Mechanical Engineers
DOE	Department Of Energy
HTE	High Temperature Electrolysis
IHX	Intermediate Heat Exchanger
LOCA	Loss Of Coolant Accident
NGNP	Next Generation Nuclear Plant
NRC	Nuclear Regulatory Commission
PCHE	Printed Circuit Heat Exchanger

NOMENCLATURE

A_{CHAN}	Cross section area of the channel, m^2
A_F	Free flow area, m^2
A_H	Total heat transfer area, m^2
c_p	Specific heat capacity at constant pressure, J/kg·K
d	Channel diameter, mm
d_m	Rectangular mapped channel diameter, mm
D_H	Hydraulic diameter, mm
f	Fanning friction factor
f_D	Darcy friction factor
h	Heat transfer coefficient, $W/m^2 \cdot K$
j	Colburn friction factor
k	Thermal conductivity
L	Heat transfer length, m
$\dot{m}$	Mass flow rate, kg/s
N_{CHAN}	Total number of channels
N_H	Number of channels along the height of the heat exchanger
N_W	Number of channels along the width of the heat exchanger
Nu	Nusselt number
p	Channel pitch, mm
P	Perimeter of the channel, m
Pr	Prandtl number
P_{IN}	Inlet pressure, MPa
Q_D	Thermal duty, MWth

Re	Reynolds number
St	Stanton number
t	Plate thickness between channels, mm
t_{eff}	Effective conduction thickness, mm
t_m	Rectangular mapped plate thickness, mm
T_{IN}	Inlet temperature, °C
T_{OUT}	Outlet temperature, °C
U	Overall heat transfer coefficient, $W/m^2 \cdot K$
V	Velocity, m/s
V_{CHAN}	Volume of space taken by channels in the heat exchanger, m^3
V_{ALLOY}	Volume of metal in the heat exchanger, m^3

Subscripts

P	Primary side of the heat exchanger
S	Secondary side of the heat exchanger

Greek

ρ	Density
σ_D	Maximum allowable stress, MPa
ΔT_{LM}	Log mean temperature difference
Δp_{fric}	Frictional pressure drop, kPa

Modeling a Printed Circuit Heat Exchanger with RELAP5-3D for the Next Generation Nuclear Plant

1. INTRODUCTION

The Next Generation Nuclear Plant (NGNP) project was initiated based on a U.S. Department of Energy (DOE) study aimed at the research and development of technologies to integrate large-scale production of hydrogen, electricity, and process heat using nuclear energy.[1] The NGNP will serve to provide the United States with an advanced energy solution through the use of peaceful nuclear technology, reduce the adverse impact on the environment caused by carbon emissions, and reduce the dependence on foreign fossil fuels. The ultimate goal of NGNP would be to build a Nuclear Regulatory Commission (NRC)-licensed nuclear plant with a large-scale hydrogen production facility. The reactor-to-process plant coupling would require efficient heat transfer along with an optimal distance between the facilities for safety considerations. An intermediate heat transport loop, using an intermediate heat exchanger (IHX), would be a necessity for satisfying minimum safety separation requirements as wells as providing maximum heat recovery. There is also the possibility of utilizing waste heat from the power production cycle for industries requiring process heat like seawater desalination. Figure 1-1 shows the schematic of the proposed NGNP system for electricity generation, hydrogen production, and other industrial applications.

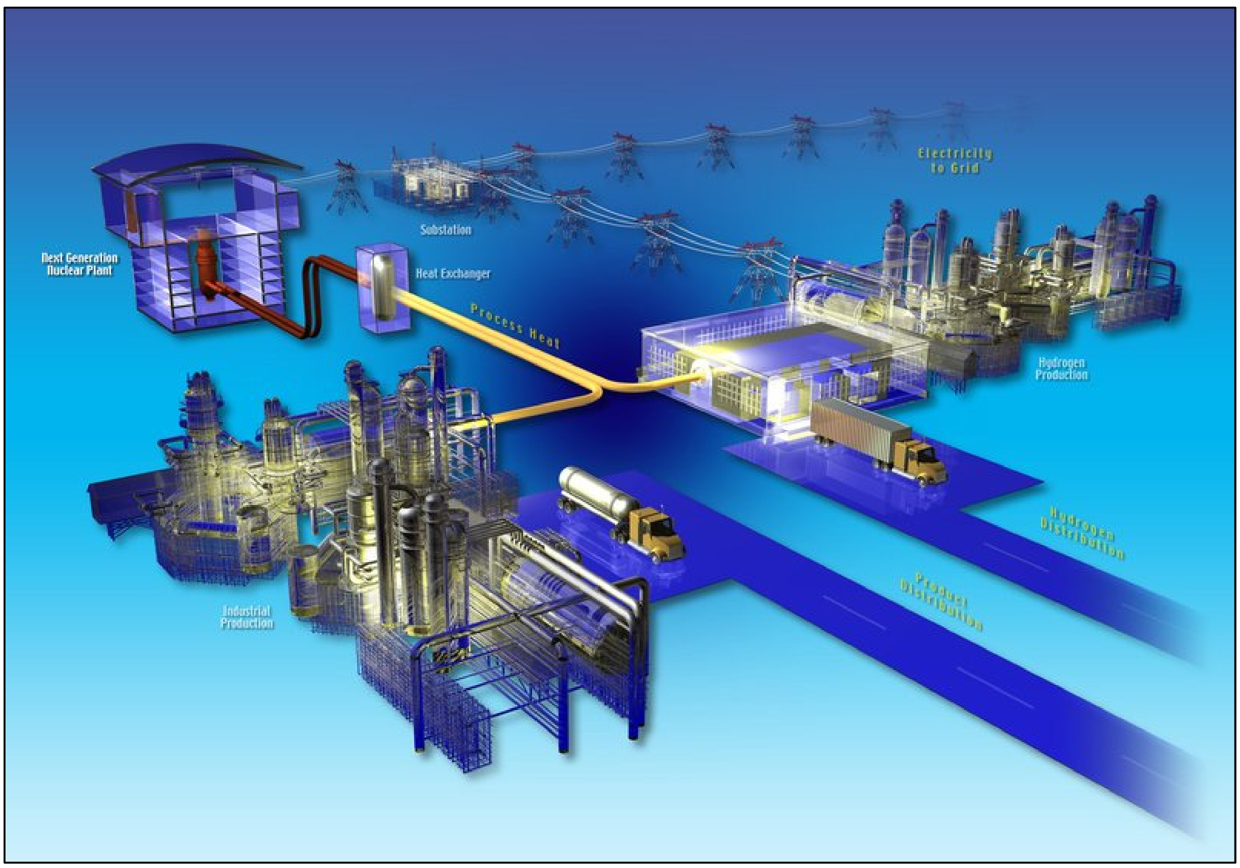

Figure 1-1. Schematic of proposed NGNP system.

The goal of NGNP is to increase energy efficiency by merging old and current technologies. Cost-effective, yet efficient and compact, heat exchangers between the nuclear plant and industrial facilities will be incorporated to maximize the transfer of energy for industrial use. The heat exchanger in question should be an equivalent Class I/Class II high-temperature component, designed in accordance with American Society of Mechanical Engineers (ASME) Boiler and Pressure Vessel Code, Sec. III. Selection of the appropriate material is paramount because the heat exchanger design will be subject to the following conditions:

- Design life of up to 60 years
- Operability in corrosive environments because of helium contamination
- Good mechanical properties: tensile strength, creep, etc.

The high temperature environment in the NGNP is challenging for many structural materials. Heatric™ recommended two materials of interest for nuclear industry: dual certified SS316/316L stainless steel and nickel-based Alloy 617.[2] At present there are no NRC-approved materials for NGNP, so Alloy 617 was selected for this study.

This study investigated a new class of compact heat exchangers called printed circuit heat exchangers (PCHE) for use in the NGNP. Compact heat exchangers have high surface area density, which translates to better heat transfer and a general reduction in size.[3] The compactness is achieved by the use of fins or, in the case of a PCHE, microchannels. A summary of compact heat exchangers has been presented in Appendix A.

PCHEs have been rated to operate under temperature range (from cryogenic to 900°C) and withstand pressures up to 60 MPa.[4] The design of PCHEs enables them to be suitable for high purity, corrosive streams and is not susceptible to flow induced oscillations and vibrations, unlike conventional shell and tube heat exchangers. At present, Heatric™ is the world's largest manufacturer of PCHEs, and their design specifications were chosen for this study. [5] According to Heatric™, PCHEs require low maintenance if used in streams with particulate size limited to 300 µm. Though PCHEs have been widely used in the oil and natural gas industry in the last two decades, the nuclear power industry is yet to adopt this technology. Over the last 10 years, much of the research is centered on estimating performance because of the scarcity of available information in PCHE design. For more details on Heatric™ heat exchangers and material properties, refer to Appendix B.

The Brayton cycle with helium as the working fluid is currently the most mature of closed gas turbine cycles. Helium (He) is one of the working fluids in the intermediate heat transport loop in NGNP under strong consideration because of the following advantages:

- Low neutron cross section makes them ideal as thermal nuclear reactor coolants
- High temperature operational tolerance for efficient power generation
- Radionuclide retention under accident conditions
- Inert nature—no metal-water or metal-air reactions
- Elimination of steam cycle and high pressure steam generators by using Brayton cycle turbine
- Potential for use in nuclear waste disposal because of harder neutron energy spectrum, resulting in more effective burning of actinides
- In-service inspections are possible because of better observability, hence greater safety assurance
- Gas-cooled fast reactor studies demonstrated that during loss of forced circulation accidents, the natural circulation of helium would provide for adequate passive cooling for reactors up to 840 MWth.

Since there is little experience in using helium in a direct cycle application in a nuclear reactor, an extensive development program is necessary for reliability purposes.

The objectives of this study were to design and model a PCHE in RELAP5-3D and perform a loss of coolant accident (LOCA) analysis.

2. PARAMETERS AND ASSUMPTIONS

There are two requisite primary parameters of interest for the design of an IHX between the reactor and the secondary loop (hydrogen processing plant, seawater desalination, etc.). These are defined by the reactor outlet temperature (heat exchanger inlet) ($T_{IN,P}$) and the maximum temperature delivered to the processing plant ($T_{OUT,S}$). The selected reactor outlet temperature for this study was 750°C. The selected process heat temperature, which is dependent on the nature of the application, was 710°C. The temperature drop across the heat exchanger was 40°C, which is reasonable. These temperatures were selected because the efficiency of hydrogen production using high temperature electrolysis (HTE) increases with higher temperatures, and there are various HTE processes that require temperatures from 300 to 900°C. The key parameters and constraints are described in Table 2-1. The NGNP was assumed to generate a thermal duty of 600 MWth and the heat exchanger was designed to transfer the entire heat duty. Helium is used as the coolant in the reactor side (primary side of the heat exchanger) and the secondary loop. The operating pressure in the primary and secondary sides was assumed to be 8.0 and 7.73 MPa respectively, with a pressure drop constraint of less than 2% pumping pressure. Velocity constraints were imposed because of limiting the flow between laminar and laminar-turbulent transition Reynolds numbers. Though having turbulent flow in channels have shown to increase the overall heat transfer, the pressure drop increases significantly to counter any advantages from increased heat transfer.

Table 2-1. Key parameters and constraints.

Parameter	Constraint
Thermal duty, Q_D (MWth)	600
Reactor outlet temperature (heat exchanger inlet), $T_{IN,P}$ (°C)	750
Heat exchanger outlet temperature, $T_{OUT,S}$ (°C)	710
IHX primary side inlet pressure, $P_{IN,P}$ (MPa)	8.0
IHX secondary side inlet pressure, $P_{IN,S}$ (MPa)	7.73
IHX primary and secondary mass flow rate (kg/s)	282
Pressure drop constraints (primary and secondary)	$<2\% \, P_{IN}$
Velocity constraints (primary and secondary) (m/s)	<35

Dostal previously provided a detailed component and system design for the NGNP direct Brayton power cycle.[6] Gezelius had provided detailed performance comparisons and estimates of different types of heat exchangers, including PCHEs for a gas-cooled fast reactor.[7] This study uses similar methodologies in getting the optimized parameters with updated correlations for calculating friction factor and Nusselt number. A direct-sizing algorithm for compact heat exchangers is currently under development.

The sizing of the heat exchangers will depend on the overall temperature difference between the outlet of the reactor core and the inlet temperature on the secondary side of the heat exchanger. The optimal design parameters used for RELAP5 modeling have been obtained from compact heat exchanger design theory detailed in Appendix A.

Davis et al. documented different plant configurations for coupling a hydrogen production facility to a nuclear reactor.[8] For reasons of simplicity, a parallel IHX configuration, such as the one shown in Figure 3-1, was selected. In a parallel configuration, the fluid having the highest temperature will be directed to the power production part of the primary loop and the remainder towards the hydrogen production plant. This method achieves higher overall efficiency.

3. DESIGN SUMMARY

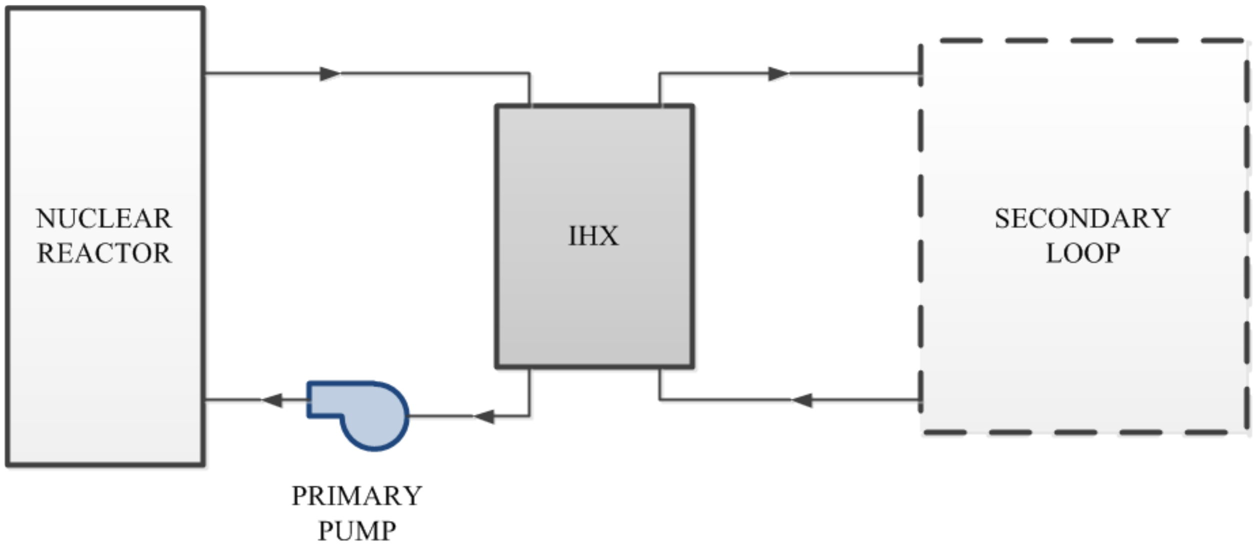

Figure 3-1. Schematic of parallel IHX configuration.

The channels for PCHE design, as shown in Figure 3-2, were defined by the parameters channel diameter (*d*), pitch (*p*), and thickness of the plate between the channels (*t*). Alternating levels of hot and cold streams were assumed. Dostal estimated the plate thickness using simplified stress calculations using maximum allowable pressure and thickness-to-diameter and pitch-to-diameter ratios.[6] The same calculations were used for the design in this report and have been summarized below.

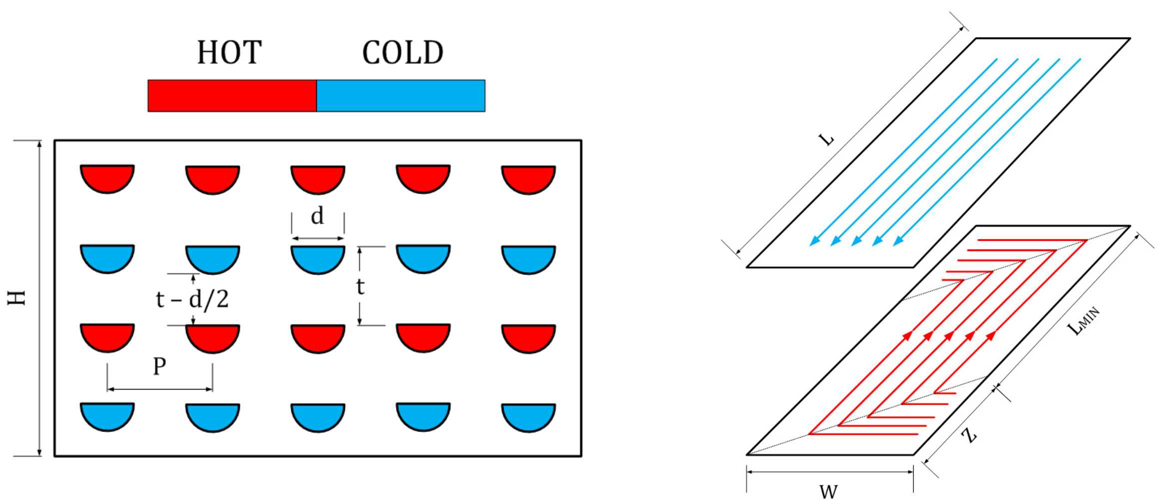

Figure 3-2. Illustration of PCHE channels with alternating hot and cold flows with the flow path.

The pitch to diameter ratio was represented as the minimum wall thickness between channels (t) and distance between the channels (p), which can be approximated as:

$$\frac{p}{d} \geq 1 + \frac{\Delta P}{\sigma_D} \tag{2.1}$$

where ΔP is the differential pressure between the hot and cold streams and σ_D is the maximum allowable stress. The maximum allowable stress was taken as 10 MPa as the design stress of Inconel 617 is 12.4 MPa at temperatures greater than 898°C.[9] A brief note on the Heatric™ PCHE and a comparison of high temperature alloys for possible application in NGNP is presented in Appendix B.

A RELAP5-3D model was developed and is illustrated in Figure 3-3. The model represents the heat exchanger as PIPE volumes (Components 330 and 390) connected by a heat structure (Component 1330). The PIPE component, which simulates the many small channels in the PCHE, has 40 volumes to provide detailed nodalizations for adequate convergence. Components 300 and 370 are the source volumes in the primary and secondary side respectively and are of type TMDPVOL (time-dependent volume) which provides the reactor and primary loop pressure and temperature. Components 310 and 375 are the time-dependent junctions used for controlling the mass flow rate into the system. Also, the time-dependent components set the boundary conditions of the problem, i.e., control system pressure and mass flow during steady-state calculations. To simulate a leak, the VALVE components—Components 325 and 335 on primary inlet and outlet and Components 385 and 395 on secondary inlet and outlet—can be used to connect a volume to the containment, which is at ambient conditions (Components 100, 101, 200, and 201). The flow direction was initialized as indicated in Figure 3-3 by the addition of sink TMDPVOL, which will have a pressure lower than the source. Typically, this pressure was found from the analytical calculations discussed later. The mass flow was set to 282 kg/s in the time dependent junction at the primary side inlet. Helium was used as the working fluid in the primary and secondary sides. As mentioned before, the LOCA transient was simulated only on the primary inlet side. The model has other VALVE components that will allow for future analysis. For steady-state analysis, the VALVES connecting the system to the ambient remain closed. The primary side time-dependent volumes are initialized with 8.0 MPa and 750°C in the source and 7.92 MPa and 340°C in the sink. Similarly, on the secondary side, the source was initialized to 7.73 MPa and 300°C and the sink at 7.64 MPa and 710°C. The ambient volumes were set to room temperature and pressure, simulating the containment room. The PIPE volumes were initialized with the source pressure and mass flow rate. The material properties for Inconel 617 were used for the heat structure. The thermal conduction between the primary and secondary side is multidimensional in reality, but was modeled as 1-D using rectangular geometry. The heat transfer area is the same as calculated by the analytical design. The Gnielinski heat transfer correlation was utilized on the primary and secondary side.

The LOCA was simulated by exponentially decreasing the pressure in the source and sink time-dependent volumes from the operating pressure to the ambient pressure.

In order to accurately map curved channels in RELAP5-3D which does not accept curvilinear objects, the semicircular channels have to be mapped to rectangular channels, resulting in a change in thickness of alloy between the channels. This is very important because of dependence of thermal conduction on the material thickness. The derived transformation equations are explained in detail in Appendix C.

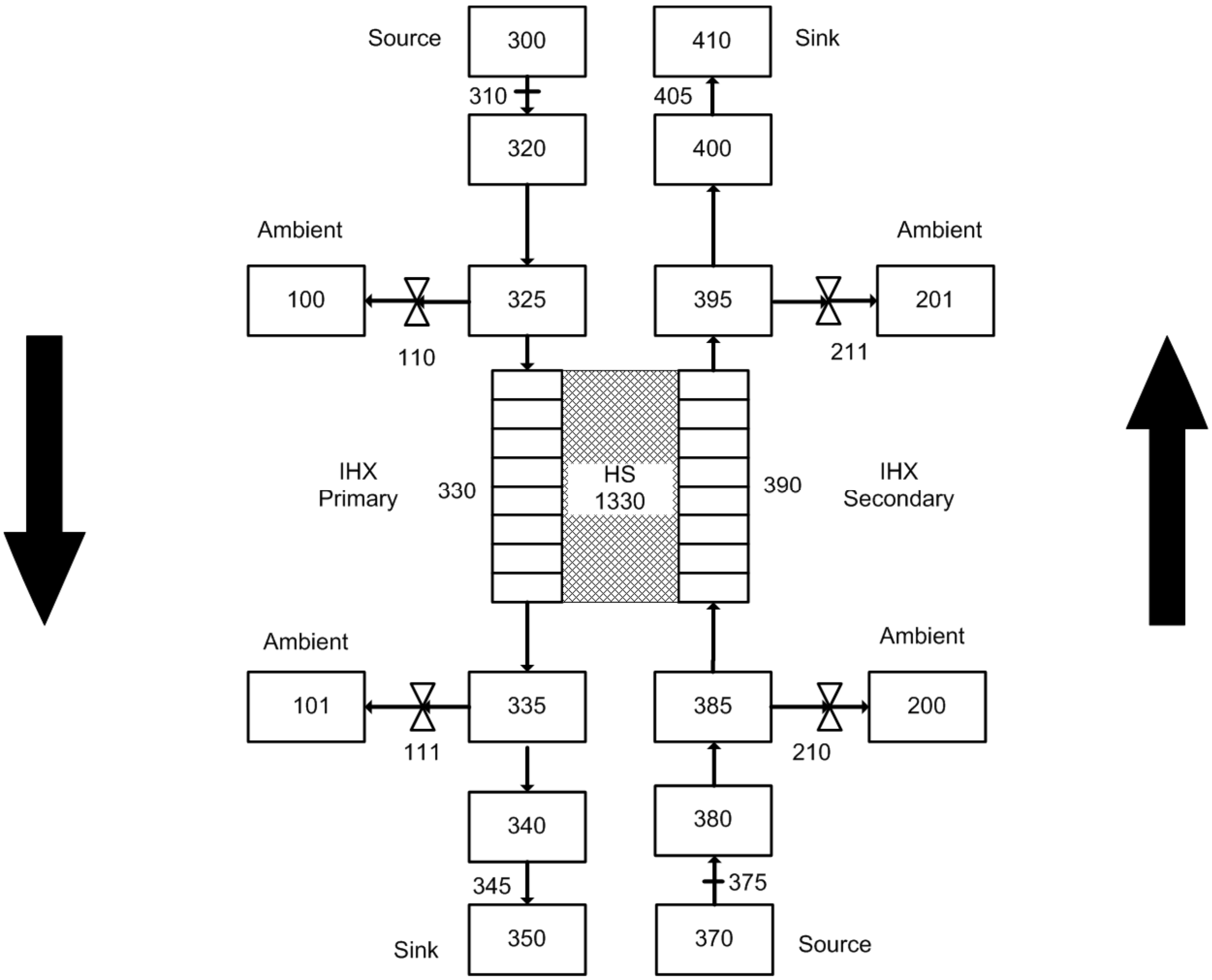

Figure 3-3. RELAP5-3D model of the PCHE.

4. RESULTS AND DISCUSSION

The heat exchanger design for use in RELAP5 was obtained using the effectiveness – number of thermal units method explained in Appendix A. The results are tabulated in Table 4-1. The calculated pressure drop required a pumping power of 9.29 MW on the primary and secondary which would result in 1.5% of the total thermal duty. The pressure drop was almost the same in both sides because of similar operating conditions. The results are comparable to available literature.[7]

Table 4-1. Heat exchanger design.

Parameter	Values
Heat transfer length, L (m)	1.475
Channel diameter, d (mm)	1.2
Channel pitch, P (mm)	1.46
Thickness of plate, t (mm)	0.96
Total no. of channels (N_{CHAN})	8.7E+06
Primary side pressure drop (kPa)	81.13
Secondary side pressure drop (kPa)	81.01
Free flow area, A_F (m^2)	2.4623
Total heat transfer area, A_H (m^2)	19,813.43
Heat transfer coefficient—Primary ($W/m^2{\cdot}K$)	1,478.15
Heat transfer coefficient—Secondary ($W/m^2{\cdot}K$)	1,559.31
Overall heat transfer coefficient, U ($W/m^2{\cdot}K$)	758.82
Total Power (MW)	600

Table 4-2 compares the design values with the results of the steady-state simulation from RELAP5-3D. The RELAP5 results show good agreement with the design calculations. The variation is ~1% of the design values, which is acceptable. The use of the Gnielinski heat transfer correlation over the default Dittus-Boelter correlation reduced the differences from 12% to less than 1%.

Table 4-2. Comparison of Design and RELAP5-3D calculated point values.

Parameter	Analytical Design	RELAP5-3D
Heat Duty (MW)	600	606
Primary Inlet Temperature (ºC)	750	744
Primary Outlet Temperature (ºC)	340	338
Secondary Inlet Temperature (ºC)	300	305
Secondary Outlet Temperature (ºC)	710	714
Reynolds number—Primary	2,104	2,170
Reynolds number—Secondary	2,185	2,219
Heat transfer coefficient—Primary	1,478.15	1,488.81
Heat transfer coefficient—Secondary	1,559.31	1,570.32

The model was next used to simulate a LOCA transient in the heat exchanger. Usually in reactors, loss of power to the pumps will result in loss of flow. Since the reactor and the secondary loop were not connected in this study, the LOCA was simulated by exponentially decreasing the pressure in the primary side of the heat exchanger.

A pipe break in the primary loop of the heat exchanger is most critical because it will result in the release of contaminants into the containment room. The break was timed to occur 25 seconds after initiation of the transient run. The primary loop pressure then exponentially decreases over the next 20 seconds until the pressure reaches ambient conditions. Figure 4-1 shows the primary loop pressure profile used to initiate the transient.

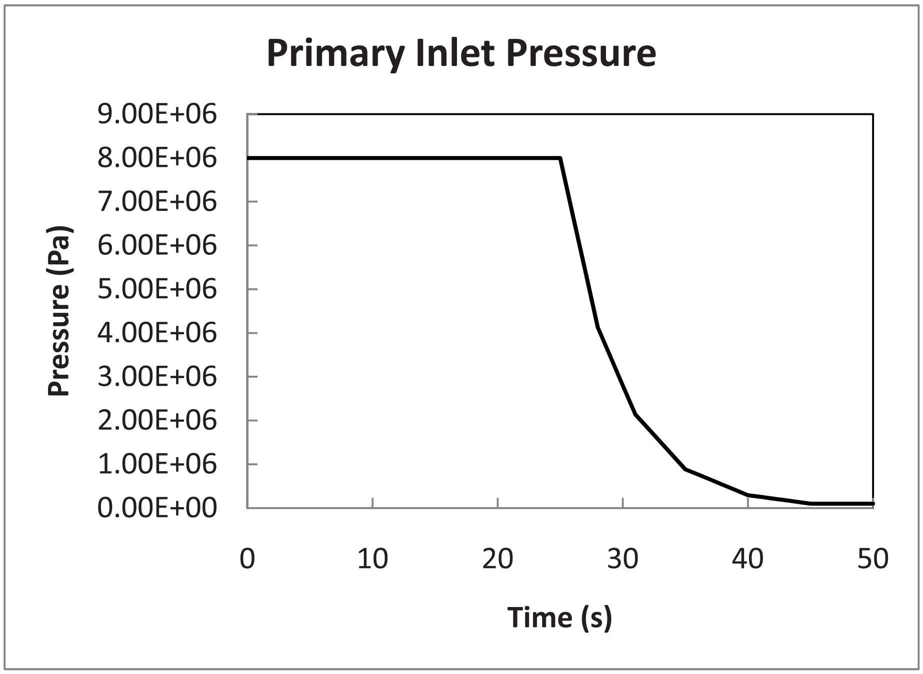

Figure 4-1. Exponential decrease in pressure at the primary loop inlet.

The helium temperature responses of the primary and secondary loops are shown in Figures 4-2 and 4-3 respectively. The primary inlet temperature decreases quickly with the loss of pressure. The small observed rise in Figure 4-2 around 35 s occurs because the primary loop temperature at the inlet decreased below the secondary loop temperature at the outlet. The primary inlet temperature then continues to decrease until it is equal to the primary outlet temperature at around 75 s.

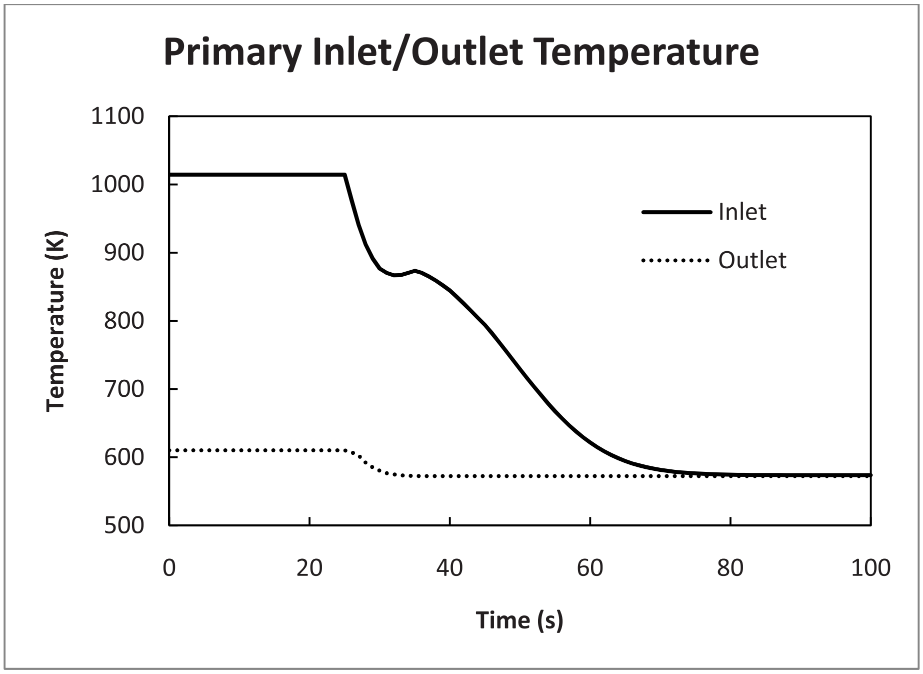

Figure 4-2. Primary loop inlet/outlet temperature response.

The secondary outlet temperature decreases steadily until it is equal to the secondary inlet temperature at around 75 s. This occurs because heat is being transferred to the now cooler primary loop.

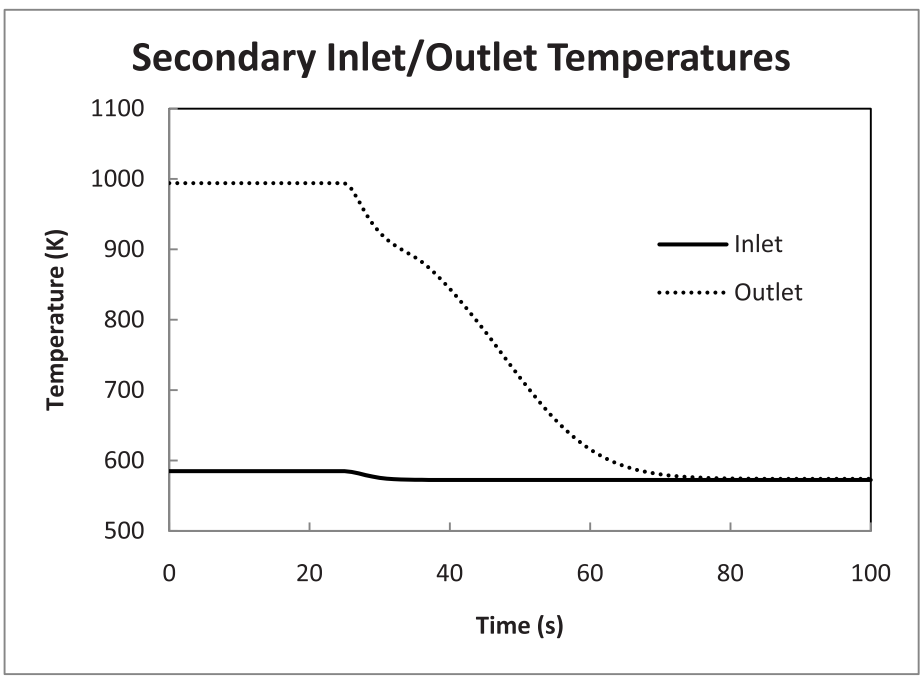

Figure 4-3. Secondary loop inlet/outlet temperature response.

The mass flow rate profile of the primary loop can be seen in Figure 4-4, it reflects the rapid coolant leak. After 45 s the mass flow rate has reduced nearly to 0.0 kg/s.

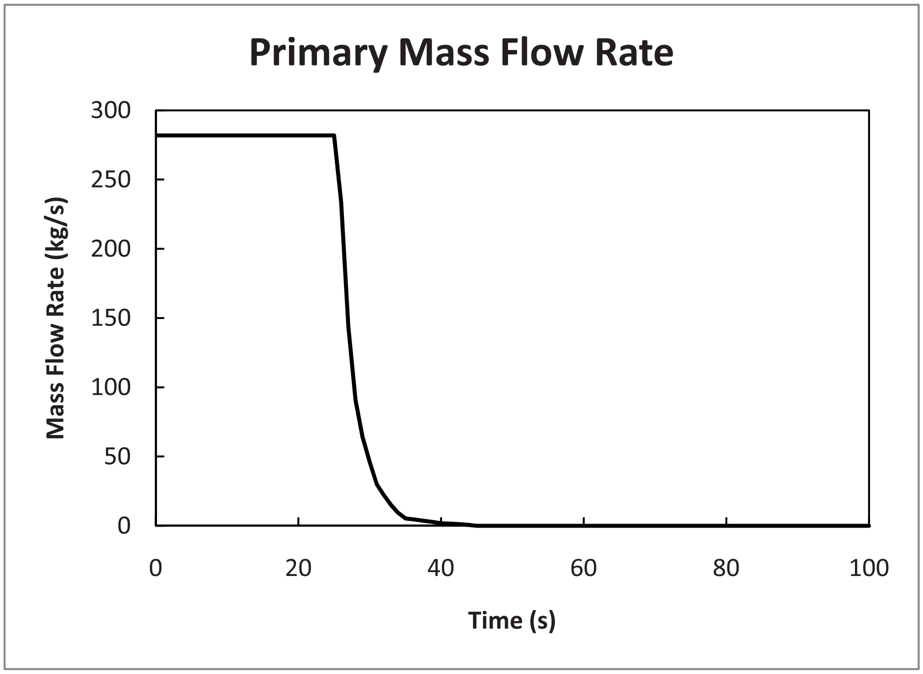

Figure 4-4. Primary loop inlet/outlet mass flow rate response.

The temperature inside the heat exchanger reacts to the loss of coolant at a slower pace. This was expected. Even if the coolant is completely lost, the residual heat in the heat exchanger takes longer to dissipate.

5. CONCLUSIONS AND RECOMMENDATIONS FOR FUTURE WORK

RELAP5 modeling of a LOCA transient was carried out on a PCHE. Using heat exchanger theory and performance relations, a heat exchanger design was developed and modeled in RELAP5. The semicircular channels were mapped into rectangular geometries and a steady-state analysis was conducted. The results of the RELAP5 steady-state analysis were in good agreement with the theoretical design. A LOCA simulation of an exponential pressure decrease at the inlet and outlet of the primary loop of the heat exchanger was performed and a catastrophic drop in pressure and mass flow was observed. The material properties of Inconel 617 were used to get accurate heat transfer coefficient results.

Several important research and development areas were identified during the course of this work, which sets the course for future work. A RELAP5 model of a high temperature gas-cooled reactor would be required to couple the heat exchanger along with the requisite turbo-machinery for an accurate depiction of the system. Likewise, detailed modeling of the secondary loop with the power conversion unit and hot/cold legs for the hydrogen production/process plant would be required to complete the design. With a complete design, the breaks could be simulated on both the primary and secondary sides, at the inlet and/or outlet. Transients analyses of the heat exchanger and power conversion unit during start up, load shifts etc. need to be carried out.

6. REFERENCES

1. P. Mills, R. Soto, and G. Gibbs, *Next Generation Nuclear Plant Pre-Conceptual Design Report*. INL/EXT-07-12967, Rev.1, November 2007.

2. X. Li, T. Smith, D. Kininmont, and S. J. Dewson, "Materials for Nuclear Diffusion-Bonded Compact Heat Exchangers," *Proceedings of ICAPP '09,* 2009, p. 9.

3. J. Hesselgreaves, *Compact Heat Exchangers: Selection, Design and Rating*. 1 ed. San Diego, CA, Pergamon, 2001.

4. X. Li, D. Kininmont, R. L. Pierres, S. J. Dewson, "Alloy 617 for the High Temperature Diffusion-Bonded Compact Heat Exchangers," *Proceedings of ICAPP '08*, 2008. p. 7.

5. X. Li, R. Le Pierres, S. Dewson, et al., "Heat exchangers for the next generation of nuclear reactors," *Proceedings of the ICAPP*, Vol. 6, 2006, pp.4–8.

6. V. Dostal, M. Driscoll, and P. Hejzlar, "A supercritical carbon dioxide cycle for next generation nuclear reactors. March 2004, p. 10.

7. K. Gezelius, "Design of compact intermediate heat exchangers for gas cooled fast reactors," *MIT-ANP-TR-103,* May 2004.

8. C. Davis, C. Oh, R. Barner, and S. D. F. Sherman, Thermal-Hydraulic Analyses of Heat Transfer Fluid Requirements and Characteristics for Coupling a Hydrogen Production Plant to a High-Temperature Nuclear Reactor, INL/EXT-05-00453, June 2006.

9. S. Dewson and X. Li, "Selection Criteria for the High Temperature Reactor Intermediate Heat Exchanger," *Proceedings of ICAPP*, Vol. 5, 2005, pp.15–19.

10. T. Kuppan, *Heat Exchanger Design Handbook*. Marcel Dekker, 2000.

11. W. Kays and A. London, *Compact heat exchangers*, New York, NY, McGraw-Hill, 1984.

12. A. Colburn, "A method of correlating forced convection heat-transfer data and a comparison with fluid friction," *International Journal of Heat and Mass Transfer*, Vol. 7, Issue 12, 1964, pp. 1359-1384.

13. V. Gnielinski, "Heat transfer and pressure drop in helically coiled tubes," *Tien C, Carey V, Ferrell J, Proceedings of the Eighth International Heat Transfer Conference,* Vol. 7. San Francisco, CA, Elsevier; 1986, pp. 2847–2854.

14. P. Linstrom and W. Mallard, *NIST Chemistry WebBook*, NIST Standard Reference Database Number 69, National Institute of Standards and Technology, Available at: http://webbook.nist.gov.

Appendix A

Compact Heat Exchangers[a]

a. This section has been condensed from Ref. 3, 11 and 12.

Appendix A
Compact Heat Exchangers

The heat exchanger design balances heat transfer characteristics of the fluids with pumping requirements for fluid transfer through the heat exchanger. For liquids, this power requirement is usually small. In the case of gases, however, it is imperative to consider the pumping power a suitable design variable because it serves as an indicator for energy requirements in heat exchanger operation. This energy requirement can be high in most thermal power systems, as mechanical energy is significantly higher in the cost of thermal energy.

The velocity of fluid flow is a very important parameter in the design process, as most flow passages would show an increase in the heat transfer per surface area with an increase in fluid velocity. But the friction-to-power expenditure is also associated with an increase in fluid velocity in the form of a drop in pumping pressure; hence, a heat exchanger design is a function of heat transfer rates and pressure drop specifications.

Different types of heat exchangers—classified on the type of performance, application, operating environment, physical characteristics, etc.—are available but outside the scope of this report. Compact heat exchangers are of primary interest to be used as the intermediate heat exchanger of the NGNP because of the following specific design characteristics reported by Kuppan[11]:

1. High heat transfer area per unit volume of the core.
2. Small hydraulic diameter (D_H).
3. Pressure drop is an important design consideration.
4. Large frontal area and a short flow length.
5. Little or no chance of fluid contamination.
6. Good for gas-to-gas applications. For preliminary design considerations, the physical dimensions may be assumed, but optimization would be necessary to ensure optimal performance. The output is usually displayed in terms of heat transfer coefficient (h), pressure drop across the heat exchanger (ΔP), number of thermal units (N), and pumping power (W). The analysis is performed for primary and secondary sides with the consequences of different cross-sectional areas, volume, and materials. The primary and secondary surfaces are invariably in transitional or fully turbulent Reynolds number regimes, and developed for pure counter-flow, but the analysis also works reasonably well for cross-flow. An overview of heat exchanger design is highlighted in this section. Detailed performance correlations for different types of surfaces are then explained and the complete thermal design and analysis of the printed circuit compact heat exchanger is discussed with an emphasis on optimization.

Kays and London described an approach to explain surface performance as functions of Reynolds number using Colburn friction factor j and Fanning friction factor f.[12] The Colburn j factor, as first described by Colburn using a power law relationship, gives heat transfer coefficient h as a function of Prandtl number Pr, and valid for transitional flows.[13]

Starting with the specified heat load, ignoring surface efficiency and wall resistance, is given as:

$$Q = \dot{m}c_p\left(T_2 - T_1\right) = hA_H\Delta T_{LM} \tag{A-1}$$

where $\dot{m}$ is the mass flow rate in kg/s, c_p is the specific heat capacity at constant pressure in J/kg·K, h is the heat transfer coefficient, A_H is the total heat transfer area in m^2, T_2 and T_1 are the temperatures in the hot and cold sides and ΔT_{LM} is the log mean temperature difference.

The Colburn factor is expressed in terms of the heat transfer coefficient as,

$$j = \frac{Nu}{RePr^{1/3}} = StPr^{2/3} \tag{A-2}$$

where Re is the Reynolds number, Pr is the Prandtl number, St is the Stanton number, and Nu, the Nusselt number, is given by

$$Nu = \frac{hD_H}{k} \tag{A-3}$$

where the hydraulic diameter $D_H = \frac{4A_{CHAN}L}{A_H}$ and k is the thermal conductivity. Also, the friction factor f is an important design parameter and depends on the surface characteristics and Reynolds number of the flow. The following equations were used to calculate the heat exchanger performance. One significant assumption is that the printed circuit heat exchanger has straight channels of semicircular cross section.

The cross sectional area A_{CHAN} and perimeter P of a semicircular channel is given by

$$\begin{aligned} A_{CHAN} &= \frac{\pi D^2}{8} \\ P &= \frac{\pi D}{2} + D \end{aligned} \tag{A-4}$$

where D is the diameter of the channel.

The free flow area A_F and heat transfer area A_H of the primary or secondary side can be evaluated from

$$\begin{aligned} A_F &= N_{CHAN} \times A_C \\ A_H &= N_{CHAN} \times L \times P \end{aligned} \tag{A-5}$$

where N_{CHAN} is the number of channels in the primary or secondary side and L is the length of the channel.

The heat transfer correlations for flow in semicircular ducts have been obtained from Hesselgreaves.[3] The hydraulic diameter is used for noncircular ducts. The Gnielinski correlation has been employed for flows in the transitional to turbulent flow regime (2300<Re<5X10^6) for smooth, straight semicircular ducts.[14]

$$Nu = \frac{\left(\frac{f}{2}\right)\left(Re-1000\right)Pr}{1+12.7\left(Pr^{\frac{2}{3}}-1\right)\sqrt{\frac{f}{2}}}, \quad 2300 \le Re \le 5\times10^6 \quad 0.5 \le Pr \le 2000 \tag{A-6}$$

where Nu is the Nusselt number, Pr the Prandtl number, Re the Reynolds number, and f is the Fanning friction factor defined by Bhatti and Shah[3] as

$$f = A + BRe^{-\frac{1}{m}} \begin{cases} \text{for} \quad 2000 \le Re < 4000 & A = 0.0064, \quad B = 2.3 \times 10^{-8}, \quad m = -2/3 \\ \text{for} \quad 4000 \le Re \le 10^7 & A = 0.00128, \quad B = 0.1148, \quad m = 3.2154 \end{cases} \tag{A-7}$$

The Gnielinski correlation has been superseded by other correlations, but has been used in this report because of the use of the correlation in RELAP5. The Darcy channel friction factor (f_D) is a very vital parameter that is also used towards calculating the frictional pressure drop, which is calculated by

$$\Delta p_{fric} = f_D \frac{4L}{D_H} \frac{1}{2} \rho V^2 \tag{A-8}$$

where L is the flow length of the channel, ρ is the density, and V is the local fluid velocity. The Fanning friction factor calculated previously is different from the Darcy friction factor. The Darcy friction factor for turbulent flow in smooth round channels is estimated from the Colebrook equation as

$$\frac{1}{\sqrt{f_D}} = 1.5635 \ln\left(\frac{Re}{7}\right) \quad 4 \times 10^3 \le Re \le 10^7 \tag{A-9}$$

In this study, the channels were in the transitional flow regime, so there would be a slight correction because of uncertainty to the correlations explained above.

NOTE: The Prandtl number and other thermophysical properties such as density, specific heat capacity, and viscosity at a given temperature and pressure can be obtained from the National Institute of Standards and Technology.[14]

Appendix B

Heatric^{TM} Printed Circuit Heat Exchanger[b]

b. This section has been condensed from the technical papers published by Heatric Division of Meggitt (UK) Limited. All images are copyrighted by Heatric and have been released for informational purposes. For the complete peer-reviewed literature pertaining to Heatric PCHEs, please refer to http://www.heatric.com/technical_papers.html.

Appendix B
Heatric^{TM} Printed Circuit Heat Exchanger

Printed circuit heat exchangers (PCHEs) were primarily developed for refrigeration applications. They are constructed by diffusion bonding a stack of plates that have been photochemically etched. The name arises from comparisons to printed circuit board construction technology. Hesselgreaves details the construction process for the Heatric^{TM} PCHE, the only organization currently involved in the manufacture of this type of heat exchangers.[3] Using a thermal soaking period to enable grain growth, it was possible to create an interface-free bond between the plates, thus giving the heat exchanger high strength and very high operating pressure capabilities. The core of a typical Heatric^{TM} diffusion-bonded PCHE is shown in Figure B-1. The photomicrograph of the cross section shown in Figure B-2 shows that the fluid passages are semicircular, typically1.0 to 2.0 mm wide, resulting in low hydraulic diameters of 1.5 to 3.0 mm.

Figure B-1. Core of PCHE with diffusion bonded plates (Courtesy: Heatric^{TM}).

Figure B-2. Photomicrograph of the semicircular passages (Courtesy: Heatric^{TM}).

Heatric^{TM} has claimed to produce units of high surface areas, >2,500 m^2, with any desired flow configuration. An example of a finished PCHE for high pressure and high temperature gas-to-gas applications is shown in Figure B-3. The presence of low hydraulic diameters is evident in the profile of the heat exchanger, which can aid high pressure duty cycles. Some of the salient features of the PCHE from Heatric^{TM} are given below:

1. PCHEs can be four to six times smaller than conventional shell-tube heat exchangers of the same duty
2. Pressure capabilities of 600 bar and temperature range from cryogenic to 900°C, making it a likely candidate for VTHR
3. High thermal effectiveness of 98% possible with a single unit
4. Multiple process streams can be incorporated in a single unit
5. The construction process uses a wide range of materials, making them suitable for corrosive and high purity streams
6. Design life of up to 60 years (life of the reactor).

Figure B-3. Typical PCHE configuration (Courtesy: Heatric™).

The limitations are the same as those of plate-fin heat exchangers, with cleaning virtually impossible in the tiny fluid passages, and design-code issues, with no nuclear approved material selection available.

Since requirements for the very high temperature reactor demand high temperatures for power generation and/or hydrogen production, the features of Heatric™ PCHEs are very appealing. Current manufacture materials include Alloy 617, Alloy 230, Alloy X and XR, Alloy 800 variants, and Alloy 602CA. Figure B-4 shows the maximum design stress for a given temperature relationship for the materials, with Alloys 617, 230, and 602CA suitable for high temperature applications; but only Alloys 617 and 230 are suitable for high pressure and temperature applications.

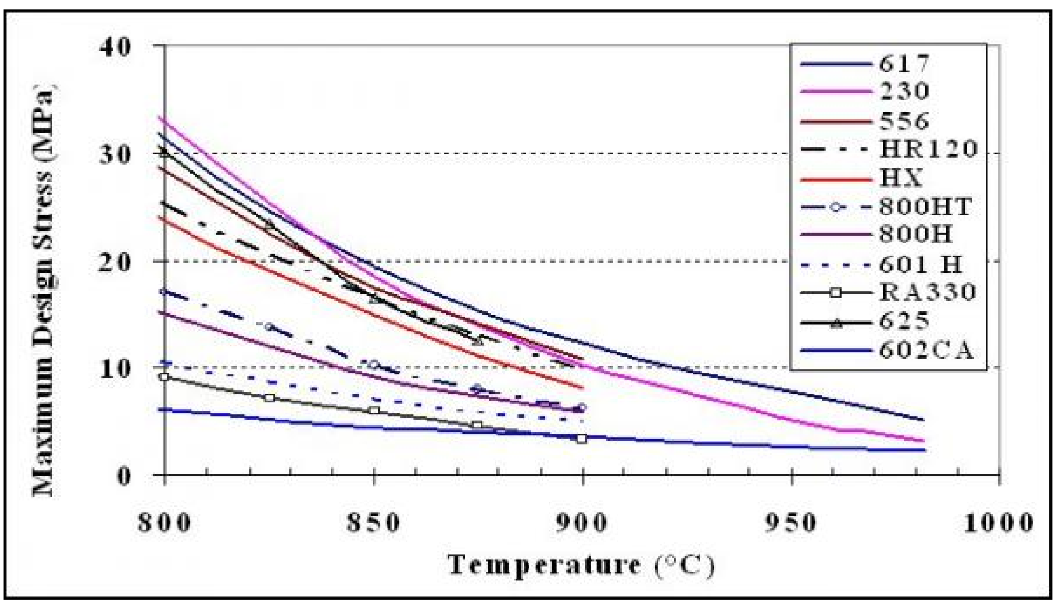

Figure B-4. Material properties for PCHE (ASME VIII I 2006).

Appendix C

Mapping of Semicircular Channels in RELAP5-3D[c]

c. This mapping technique was implemented by Mr. Cliff B. Davis and has been used in this work with his permission.

Appendix C
Mapping of Semicircular Channels in RELAP5-3D

The following equations were used to transform semicircular channels into rectangular channels for developing the input deck of RELAP5-3D. Transforming the channels from semicircular channels to rectangular will result in a change in the amount of metal present for heat transfer. Figure C-1 is an illustration of the parameters used in the mapping technique. For analysis, counter flow arrangement is assumed.

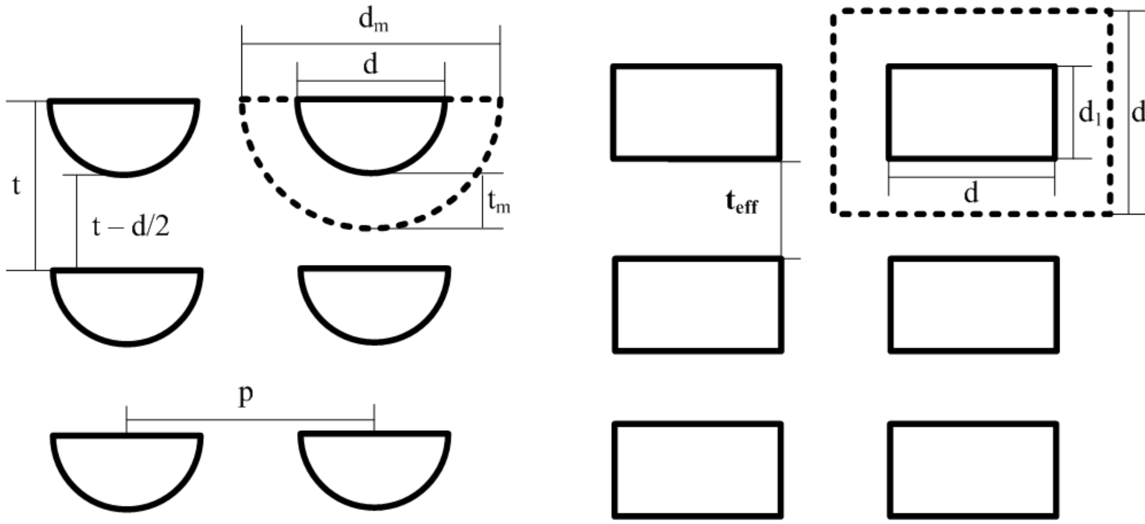

Figure C-1. Mapping a semicircular domain to a rectangular domain.

Let W, H, and L be the width, height and length of the heat exchanger respectively. The number of channels along width and height, given by N_W and N_H respectively, are defined as

$$N_W = \frac{W}{p}; N_H = \frac{H}{t} - 1 \tag{C-1}$$

where p is the pitch, t is the plate thickness, and the total number of channels can be defined as $N_{CHAN} = N_W \times N_H$.

The cross sectional channel area of the semicircular channels, $A_{CHAN} = N_{CHAN}\left(\frac{\pi d^2}{8}\right)$.

Volume of space taken by the channels, $V_{CHAN} = A_{CHAN} \times L$.

Volume of alloy in the heat exchanger, $V_{ALLOY} = (W \times L \times H)_{HX} - V_{CHAN}$.

Assuming the plate as a thick walled cylinder with an inner radius $\frac{d}{2}$ and outer radius as the thickness of the plate (t) the area of metal available for heat transfer per channel is given by

$$\left(A_{ALLOY}\right)_{Annulus} = \frac{V_{ALLOY}}{N_{CHAN} \times L_{HX}} = \frac{\pi\left(d_m^2 - d^2\right)}{8} \tag{C-2}$$

where d_m is an arbitrary diameter as illustrated in the semicircular channels in Figure C-1.Similarly, the arbitrary thickness, t_m as illustrated in the Figure C-1, is defined as

$$t_m = \frac{1}{2}\left(d_m - d\right). \tag{C-3}$$

The rectangular mapping is illustrated in Figure C-1, with the addition of a new parameter d_1, which can be found out by the area of the rectangular channel, the same as the area of the semicircular channel as

$$A_{RECT} = A_{ANNULUS} \Rightarrow d_1 \times d = \frac{\pi d^2}{8} \Rightarrow d_1 = \frac{\pi d}{8} \tag{C-4}$$

Likewise d_m and t_m for the rectangular mapping can be found by

$$A_{ALLOY} = \left(p \times d_m\right) - \left(d \times d_1\right) \Rightarrow d_m = \frac{A_{ALLOY} + \left(d_1 \times d\right)}{p} \Rightarrow t_m = \frac{1}{2}\left(d_m - d_1\right). \tag{C-5}$$

The physical conduction thickness of the metal between channels varies along the circumference of the semicircular channel, i.e. $t \le x \le \left(t - \frac{d}{2}\right)$ so the effective thickness can be calculated as the mean of the limits given by

$$t_{eff} = \bar{t} \approx \frac{t + t - d/2}{2} = t + \frac{d}{4} \tag{C-6}$$

This effective conduction thickness will be used to modify the volumetric heat capacity of Inconel 617 alloy to preserve the thermal capacitance of the heat structure component in RELAP5-3D.